Research Article

Liquid Phase Oxydehydration of Glycerol to Acrylic Acid over Supported Silicotungstic Acid Catalyst: Influence of Reaction Parameters

Sarawalee Thanasilp[1]*, Johannes W. Schwank[2], Vissanu Meeyoo[3], Sitthiphong Pengpanich[3] and Mali Hunsom[1]

[1]*Fuels Research Center, Department of Chemical Technology, Faculty of Science, Chulalongkorn University, 254 Phayathai Road, Bangkok 10330, Thailand.*
[2]*Department of Chemical Engineering, College of Engineering, University of Michigan, Ann Arbor, Michigan, USA*
[3]*Department of Chemical Engineering, Mahanakorn University of Technology, Bangkok, Thailand*
[*]*Correspondence author. Email address: sarawalee.t@gmail.com*

Received December 8, 2014; Accepted April 17, 2015

Abstract

The liquid phase catalytic oxydehydration of glycerol to acrylic acid over supported silicotungstic acid (SiW) catalysts was carried out in the batch reactor. The effect of oxidizing agent concentration (H_2O_2), reaction temperatures (70 and 90 °C), types of supports (HZSM-5, SiO_2 and Al_2O_3) and SiW loading (20-60 wt.% based on support) on the conversion and product yield were investigated. The addition of H_2O_2 and supported SiW catalysts significantly conducted the synergetic positive effects on glycerol conversion and acrylic acid yields as well as other desired products including glycolic acid, formic acid, acetic acid, acrolein and acrylic acid. High reaction temperature was able to enhance high glycerol conversion as the same yield of all desired products. The BET surface area of supported SiW catalysts played much more important role in the activities of oxydehydration of glycerol that this oxydehydration was more remarkable than the acidity of catalysts. Among all supported SiW catalysts, the SiW/HZSM-5 with SiW loading of 30 wt.% exhibited the highest glycerol conversion (85.54%) with the production acrylic acid yield of 30.57 % over 2.74 M H_2O_2 at 90 °C. The kinetics of glycerol conversion to desired products over supported SiW catalyst was explored.

***Key Words*:** Glycerol; Oxydehydration; Silicotungstic acid; Acrylic acid; Support

Introduction

Due to the decrease of fossil based energy resources, the attempt to replace the petroleum resources by biomass resources has been increasingly focused on the production of both liquid fuel and petrochemical feedstock (Tsukuda et al., 2007; Witsuthammakul and Sooknoi, 2012).Biodiesel is an alternative renewable fuel that has become widely used as a partial replacement for diesel derived from non-renewable fossil fuel. It is resulting from its sustainably renewable nature, low toxicity, high cetane number, lubricity, flash point and biodegradability (Smith et al., 2009). Biodiesel is produced from the transesterification of vegetables oil or animal fat with alcohol in acid catalysts (Liu and Wang, 2009; Demirbas, 2009). This process gives glycerol as the main by-product. Approximately 100 kg of glycerol is generated from the production of 1,000 kg of biodiesel. Although large amount of glycerol is continually produced, its current demand remains unchanged. Despite an effort to utilize glycerol as alternative fuel, its combustion emits several types of toxic gases (Guo et al., 2009). Thus, many reports attempted to convert glycerol to more valuable chemicals

ISSN 1905-9159

such as propanediol (Deckwer, 1995; Huang et al., 2009; Van de Vyver et al., 2010; Gong et al., 2010; Kongjao et al., 2011; Lee and Moon, 2011), synthesis gas (Simonetti et al., 2007; Sabourin et al., 2009; Kunkes et al., 2008; Markov et al., 2011; Ghosh et al., 2012), acrylonitrile (Chieregato et al., 2012; Shen et al., 2012), liquid fuels (Henao et al., 2009; Li et al., 2012; Zakaria et al., 2012; Beatrice et al., 2013), acrolein (Shen et al., 2012; Deleplanque et al., 2010; Ulgen and Hoelderich, 2011), and acrylic acid (Witsuthammakul and Sooknoi, 2012; Deleplanque et al., 2010).

Acrylic acid is one of most interesting and important chemicals that is commonly used in adhesive, paint, plastic and rubber synthesis. Approximately 85% of the acrylic acid is produced by captive oxidation of acrolein (Etzkorn et al., 2002). Besides, acrylic acid can be produced from glycerol via the sequential step of dehydration (Ning et al., 2008; Akiyama et al., 2009) and oxidation, known as the oxydehydration reaction. According to this reaction, the water and oxygen molecules in glycerol structure are eliminated by using appropriate catalysts. The use of zeolite (HZSM-5, HBeta, HMordenite and HY) and vanadium-molybdenum mixed oxides (V-Mo, 15-70 mol.% V) were utilized as catalysts for direct conversion of glycerol to acrylic acid and these catalysts were successfully performed in the integrated dehydration-oxidation bed system (Witsuthammakul and Sooknoi, 2012). Over the acid zeolites, acrolein and acetol were mainly generated, together with acetaldehyde, propionaldehyde, pyruvaldehyde and other oxygenates as secondary products. A complete conversion of glycerol with high selectivity to acrolein (up to 81 mol %) can be obtained when medium pore zeolites (HZSM-5) and low glycerol concentration (1.37-5.50 M) were used. A separated-sequential bed system provides high selectivity for acrylic acid with small amount of acetic acid and acetaldehyde (~15 mol %). The catalyst with high vanadium content promotes total oxidation of the dehydrated products to CO while that with highly dispersed V-Mo-O phases affords 98% selectivity to acrylic acid with 48% acrolein conversion. By using W-V-O bronzes, the presence of V conferred to the catalyst the redox properties for the partial oxidation of acrolein into acrylic acid. Approximately 25% of acrylic acid yield was obtained (Chieregato et al., 2012). When Nb is incorporated, the acrylic acid yield increased up to 34% because the incorporation of Nb^{5+} led to a lower surface density of acid sites but to a greater fraction of stronger sites, which can enhance the catalytic activity and also stability of catalytic performance during short-term lifetime experiments. In the presence of Mo/V and W/V oxide catalysts in fixed bed reactor (Shen et al., 2014), some acid sites on Mo/V and W/V oxide catalysts catalyzed the glycerol dehydration to acrolein and acetaldehyde. The metallic cations with low valences in Mo/V and W/V oxide catalysts gave high oxidation activity for the formation of acrylic acid, acetic acid, CO, and CO_2. Recently, many literatures attempted to use the polyoxometalate (POM) or POM-based compounds as a catalyst for converting glycerol to acrolein or acrylic acid because it has strong Brönsted acids, high thermal stability and solubility in polar solvents such as water and alcohols, less harmful to the environment than mineral acids and its high oxidative ability (Kozhevnikov, 1995). Typically, the catalytic activity of POM catalyst depends onvarious factors such as types of POM, size of utilized support (Tsukuda et al., 2007), stability of the POM (Shen et al., 2012), the POM acidity (Lili et al., 2008). The use of POM compounds including $H_3PW_{12}O_{40}$, $FePO_4$, Mo_3VO, MoVTeNbO, W_3VO as the catalyst in gas phase reaction demonstrated the satisfactory performances on obtaining acrylic acid directly from glycerol (Deleplanque et al., 2010). Among all utilized catalysts, the $FePO_4$ provided a highly active and selective towards acrolein. Glycerol conversion was nearly complete and acrolein yields around 80-90% after 5 h of the test. The chemical equation for the glycerol oxydehydration to acrylic acid catalyzed by supported SiW catalysts is suggested as Scheme 1.

In a previous study (Thanasilp et al., 2013), we reported that various higher market value products were generated in the liquid phase oxydehydration of glycerol via Al_2O_3-supported POM catalysts at 90 °C, such as glycolic acid, propanediol, formic acid, acetic acid, and acrolein. The best yield of acrylic acid obtained with $SiW/A_{l2}O_3$ was 25%. In the current work, we continued our work with supported SiW catalyst, in order to achieve a higher glycerol conversion and product yield. The aim of this study wasto investigate the influence of oxidizing agent, reaction temperature, supported types, SiW loadings to oxydehydration reaction. The kinetic studies of the best catalyst were also examined.

$$\underset{\text{Glycerol}}{C_3H_8O_3} + \underset{\text{Hydrogen peroxide}}{H_2O_2} \xrightarrow[\text{Heat}]{\text{Catalysts}} \underset{\text{Acrylic acid}}{C_3H_4O_2} + \underset{\text{Water}}{3H_2O}$$

Scheme 1 Chemical equation for the glycerol oxydehydration to acrylic acid catalyzed by supported SiW catalysts.

Materials and methods

Catalyst preparation and characterization

SiW ($H_4SiW_{12}O_{40}.xH_2O$) was impregnated on three commercial supports including Al_2O_3 (Sigma-Aldrich, USA), SiO_2 (CARiACT Q30., Fuji Silycia Chemical, Japan) and HZSM-5 (SiO_2/Al_2O_3 = 25) (Zibo xinhong chemcial trade, China) by the incipient wetness impregnation method. A prescribed amount of 2.14 g of SiW was dissolved thoroughly in 5 ml distilled water at room temperature. Then, approximately 5 g of required support was added slowly into the solution. The obtained slurry was stirred at constant rate of 200 rpm at room temperature for 1 h. The ready-to-use supported SiW catalysts were obtained after drying at 110 °C and calcination at 400 °C for 20 h.

The BET surface area, pore volume, and average pore diameter for fresh catalysts were derived from N_2 adsorption isotherms measured at -196 °C (Micromeritics ASAP 2020). Prior to the measurement, each sample was degassed at 200 °C for 4 h. The average pore diameter was calculated according to the BJH method. The phase structure of the catalysts was determined the powder X-ray diffraction patterns (XRD) of the catalysts on a Siemens PE-2004 X-ray diffractometer using CuKa (λ = 0.15406 nm) radiation operated at 40 kV and 20 mA. The acidity of all supported SiW catalysts was determined by temperature-programmed desorption of ammonia (NH_3-TPD) in a fixed-bed continuous flow microreactor at atmospheric pressure equipped with TCD detector.

Catalytic activity test

Catalytic oxydehydration of glycerol to acrylic acid was carried out in liquid phase system at low temperature and ambient pressure. The concentration of H_2O_2 (Fisher, USA) was varied from 1.37-6.85 M. Initially, 30 ml of 20 wt.% aqueous glycerol solution (99.5% (v/v), Fisher)) was mixed with preferable quantity of supported SiW catalyst (0.30 g for 4 wt.%) in a 500 ml three-neck round bottom flask equipped with a reflux condenser and stirrer. Consequently, the temperature of the system was raised to desired temperature (70 or 90 °C) by an external electrical heater. When the required temperature was achieved, H_2O_2 was added slowly in the three-neck reactor. The reaction was monitored by sampling the liquid sample of around 1.0 ml at particular time intervals until 4 h. To terminate the reaction, all liquid samples were collected in an ice-water trap at temperature of 0-5 °C and then centrifuged on Hermle Z206A Digital Laboratory Centrifuge to separate the solid catalyst from the aqueous product. The composition of product was quantitatively analyzed by high performance liquid chromatography (Waters 410 HPLC controller) equipped with a refractive index detector in series. A Phenomenex Luna 5 μm C18 (2) 100 (25 cm×4.6 mm) was used as separating HPLC column. The net glycerol conversion, the product yield of selected products as well as the carbon selectivity were calculated on the basis of Eqs. (1) - (3), respectively:

$$\text{Glycerol conversion}(\%) = \frac{\text{C mole of glycerol converted}}{\text{C mole of glycerol initilialy added}} \times 100 \quad (1)$$

$$\text{Product yield}(\%) = \frac{\text{C mole of glycerol converted to each product}}{\text{C mole of glycerol initially added}} \times 100 \quad (2)$$

$$\text{Carbon selectivity}(\%) = \frac{\text{C mole of glycerol converted to all desired products}}{\text{C mole of glycerol converted}} \times 100 \quad (3)$$

where C is carbon.

Results and discussion

Effect of oxidizing agent and operating temperature

Table 1 summarizes the glycerol conversion and yield of various products from glycerol oxydehydration over SiW/Al_2O_3 catalysts at 240 min with SiW loading of 30 wt.% catalyst at temperature of 70 and 90 °C in the absence and the presence of H_2O_2. The use of H_2O_2 had a positive effect onglycerol conversion and yield of measured products. At 70 °C, the presence of 2.74 M H_2O_2 can enhance the increase of glycerol conversion from 9.07 to 64.30%, approximately 7.09-fold increasing, and also increasing the yield of glycolic acid, formic acid, acetic acid, acrolein and acrylic acid of 15.64, 17.97, 21.04, 3.53 and 23.51-fold, respectively. In addition, it can reduce the production of other products observing from the carbon selectivityof around 13.67-fold. That is, the carbon selectivity increased from 3.86 to 52.76% when H_2O_2 was added into the reaction, indicating the decrease of glycerol conversion to undesired products from 96.14 to 47.24%. The similar positive effect of H_2O_2 on glycerol conversion and product yield was also observed at higher temperature, 90 °C. That is, the glycerol conversion increased from 17.84 to 83.78%, when H_2O_2 at 2.74 M was introduced. This can be explained by the fact that H_2O_2 is the reactive oxygen donor providing the ideal conditions for oxidation of glycerol to glycerol aldehyde, an intermediate for glyceric acid in liquid phase (Atia et al., 2008). Further raising the amount of H_2O_2 to 6.85 M at 90 °C can enhance a more glycerol conversion up to 93.87 %. However, the presence of such high H_2O_2 concentrations could lead to dangerous reaction conditions. Therefore, for safety reasons, the reaction was carried out with H_2O_2 at 2.74 M. Nevertheless, the presence of only H_2O_2 cannot promote the progress of the oxydehydration reaction. The conversions of

Table 1 Effect of H_2O_2 content and temperature on the performance of glycerol oxydehydration over SiW/Al_2O_3 catalysts at 240 min.

Concentration of H_2O_2 (M)	Temperature (°C)	SiW loading (wt.%)	Glycerol conversion (%)	Product yield (%)					Carbon selectivity (%)[a]
				Glycolic acid	Formic acid	Acetic acid	Acrolein	Acrylic acid	
0	70	30	9.07	0.64	0.34	0.77	1.46	0.65	3.86
0	90	30	17.84	1.11	0.93	1.37	3.35	1.17	7.92
2.75	70	30	64.30	10.01	6.11	16.20	5.16	15.28	52.76
2.75	90	30	83.78	15.34	7.90	18.83	5.44	25.11	72.62
6.85	90	30	93.87	11.22	10.31	23.43	2.79	17.86	65.62
2.75	70	0	6.71	0.11	0.40	0.44	0.08	0.39	15.94
2.75	90	0	9.27	0.29	0.52	0.55	0.16	0.67	26.98

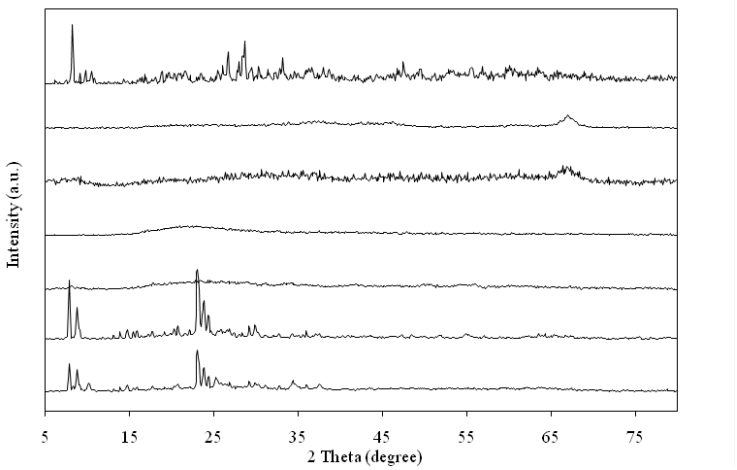

Figure 1 XRD patterns of SiW and supported SiW catalysts at 30 wt.% SiW loading (◆ SiW hexahydrate and ● HZSM-5).

glycerol were proceeded only 6.91 and 9.27% at the reaction temperature of 70 and 90 °C, respectively (Table 1). Less than 1% of desired products were generated at such condition. This indicates that the presence of H_2O_2 and SiW catalysts had the positive synergetic effect on glycerol conversion and product yields.

As also demonstrated in Table 1, in the presence of H_2O_2 at 2.74 M, raising the reaction temperature from 70 to 90 °C resulted in the raise of glycerol conversion of approximately 1.30-fold. The yield of all desired products significantly increased, especiallythe yield of acrylic acidincreased from 15.28 to 25.11 %. Besides, the generation of undesired product, diagnosing from the carbon selectivity, essentially decreased from 72.62 to less than 52.76 %. The increase in glycerol conversion in high temperature was due to high dehydration rate of glycerol in the presence of polyoxometalate catalysts, consistent with the previous report (Shen et al., 2012). The high yield of acrylic acid was due to high kinetics of acrolein oxidation to acrylic acid (Tichy, 1997), resulting in the low generation of undesired products. However, the temperature higher than 90 °C was not performed due to it required a proper controlling system, which is impractical in operation.

Effect of supports

Three types of support were utilized in this work including Al_2O_3, SiO_2 and HZSM-5. Figure 1 reveals the XRD pattern of unsupported SiW catalyst and all supported SiW catalysts at the loading of SiW on support of 30 wt.%. The XRD pattern of SiW shows the crystalline phase at 2θ of 27.3°, assigning to the SiW hexahydrate (Tsukuda et al., 2007). For SiW/SiO_2 and SiW/Al_2O_3 catalysts, no characteristic peaks assigning to the utilized SiW were observed, suggesting that SiW catalysts were

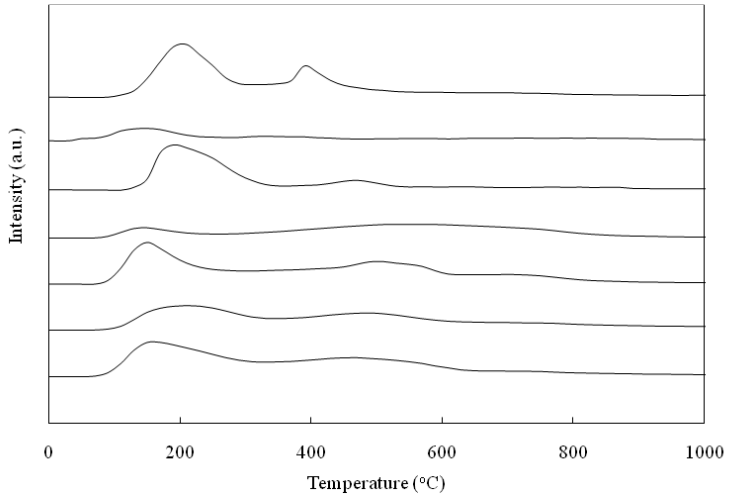

Figure 2 NH_3-TPD profiles of supported SiW catalysts and their supports at 30 wt.% SiW loading

highly dispersed on the support. In case of SiW/HZSM-5 catalyst, the detected reflections were similar to that of SiW support, implying the presence of the cubic SiW hexahydrate phase on the structure of such catalyst.

Textural properties for supported SiW catalysts immobilized on Al_2O_3, SiO_2 and HZSM-5 supports derived from N_2 physisorption isotherms are summarized in Table 2. The BET surface area of utilized supports was in an order of HZSM-5 > Al_2O_3> SiO_2, while the inverse order was observed in their pore volumes. The pore diameter changed in the order of Al_2O_3> HZSM-5 > SiO_2. When SiW was impregnated on the support surface, the similar trend of change of BET surface area, pore volume and average pore diameter was observed. However, the BET surface area, pore volume as well average pore diameter of all supported SiW catalysts decreased significantly compared to the original SiW-free supports. The decrease in BET surface area may be attributed to the support pores blocking by catalyst particle. This is because the pores of Al_2O_3, SiO_2 and HZSM-5 are 5.46, 2.89 and 4.32 Å and the Keggin unit diameter is 12~Å (Popa et al., 2005). Thus, it is reasonable to say that the pores are blocked by the active phase.

The surface acidity of all utilized supports and supported SiW catalysts determined by NH_3-TPD analysis isshown in Figure 2. Theoretically, the acid sites are classified as weak- (150-300 °C), medium- (300-500 °C) and strong- (500-650 °C) strength (Chino and Okubo, 2005). Two desorption peaks at 203 and 388 °C were observed for unsupported SiW, indicating the presence of weak- and medium-strength acid sites on the surface of this catalysts. No sharp desorption peaks were observed for all utilized supports, they appeared as a board peaks. For supported SiW catalysts, two broad NH3-TPD peaks was observed at the temperature of 161 and 522 °C and 191 and 469 °C for SiW/HZSM-5 and SiW/Al_2O_3 catalysts, respectively, indicating the presence of weak- and strong-strength acid sites in their structures. Peaks appeared at 154, 491 and 735 °C were observed on the NH_3-TPD profile of SiW/SiO_2 catalysts, denoting the presence of weak-, medium- and strong-strength acid sites on its structure. Compared with the desorption peaks of the unsupported SiW catalyst, the NH_3-TPD peaks of all supported SiW catalysts shifted to low temperature and loss some intensity, indicating a weakening of the acid site due to interactions with their supports. Upon supporting SiW on all supports, the medium-strength peak loss most of intensity but appeared to shift toward higher temperature (~480 °C).

The amount of acid sites of all supported SiW catalysts was calculated from NH_3-TPD desorption peak area and summarized in Table 2. The total acidity of the supported SiW catalysts was in an order of SiW/Al_2O_3 > SiW/HZSM-5 > SiW/SiO_2. The acidity of all supported SiW catalysts was lower than that of unsupported SiW catalyst. However, it was still greater than that of fresh Al_2O_3, SiO_2 and HZSM-5 supports. This is because the addition of POM did not introduce any new acid sites on support surface, but led to a replacement by other acidic sites (Atia et al., 2008; Chino and Okubo, 2005). The weak interaction of support with the SiW catalyst kept its Brønsted acid character and led to an increased proportion of medium- and strong-strength acid sites. In this case, a portion of the SiW lost its acidity due to the distortion of the Keggin structure.

Table 2 Textural properties and surface chemistry of supported SiW catalysts and the corresponding supports

Catalysts	Textural properties			Surface chemistry	
	BET surface area (m^2/g)	Pore volume (cm^3/g)	Average pore diameter (Å) (mmol NH_3/g Cat.)	Acid amount	Total acidity (mmol NH_3/g Cat.)
SiW	121.5	0.357	3.74	2.88 (108-303 °C)	3.81
				0.93 (351-439 °C)	
Al_2O_3	267.8	0.229	5.46	0.50 (46-275 °C)	0.68
				0.18(275-453 °C)	
SiO_2	223.6	0.835	2.89	0.28 (71-229 °C)	0.85
				0.57 (248-921 °C)	
HZSM-5	289.4	0.173	4.32	0.71 (81-349 °C)	0.97
				0.25 (362-640 °C)	
SiW/Al_2O_3	214.6	0.128	4.11	1.19 (110-356 °C)	1.42
				0.23 (390-543 °C)	
SiW/SiO_2	201.2	0.644	2.08	0.78 (56-312 °C)	1.24
				0.42 (375-610 °C)	
				0.04 (617-906 °C)	
SiW/HZSM-5	233.4	0.153	2.62	0.88 (46-342 °C)	1.31
				0.43 (355-669 °C)	

[a]SiW/HZSM-5 catalyst at 90 °C and 30 wt.% SiW loading after 6 times used.

Figure 3 shows the variation of glycerol conversion and product yield as a function of time from glycerol oxydehydration over supported SiW catalysts at identical SiW loading of 30 wt.%, reaction temperature of 90 °C and ambient pressure. A similar pattern of the glycerol conversion and product yield was appeared in the presence of all supported SiW catalysts. Glycerol conversion increased initially with the increasing reaction time and then leveled off at reaction times longer than 120 min. With regards to the variation of product yield, the yields of acetic acid, glycolic acid and formic acid increased slightly with increasing reaction time. The yield of acrylic acid was low during the first 30-120 minutes of reaction time, while a high yield of acrolein was obtained during the same period. However, at longer reaction times, the yield of acrolein decreased, whilst the yield of acrylic acid increased. This implies that acrolein was oxidized to acrylic acid in the presence of supported SiW catalysts.

Consider at long reaction time (240 min), as summarized in Table 3, the glycerol conversion and yield of desired products were ranked in the order of SiW/HZSM-5 > SiW/Al_2O_2> SiW/SiO_2. Less than 16% of converted carbons were transformed to the undesired products in the presence of SiW/HZSM-5 catalyst. These suggest that the SiW/HZSM-5 catalyst was more active than the other two types. Although SiW/HZSM-5 catalyst had lower acid strength than SiW/Al_2O_3catalyst, it gave higher glycerol conversion under the same operating conditions. The trend of catalytic activity of supported SiW catalysts for the oxydehydration of glycerol was a good coincidence with the trends of BET surface area, but not the acidity, pore volume and average pore diameter of corresponding catalysts (Table 2). This suggests that the dehydration of glycerol over supported SiW catalysts required the acidity just a certain value and then the BET surface area played an important role. The catalyst with high BET surface area and appropriate acidity allowed a more available area for glycerol adsorption, which can further undergo dehydration to intermediate/product species. This hypothesis is supported by the low BET

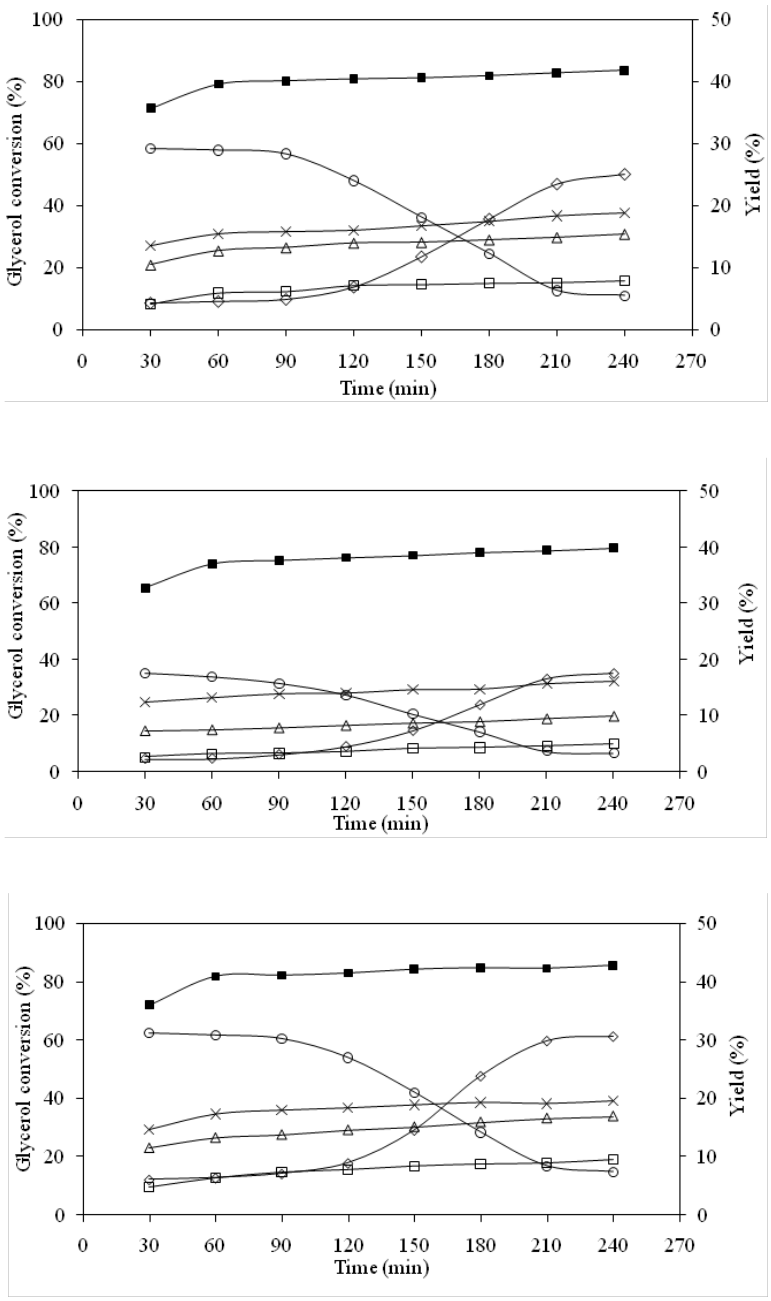

Figure 3 Variation of (■) glycerol conversion and yields of (△) glycolic acid, (□) formic acid, (✕) acetic acid, (○) acrolein and (◇) acrylic acid as a function of time over (a) SiW/Al_2O_3, (b) SiW/SiO_2 and (c) SiW/HZSM-5 at 90 °C and 30 wt.% SiW loading.

Table 3 Effect of supports on the performance of glycerol oxydehydration over supported SiW catalysts at SiW loading of 30 wt.%, temperature of 90 °C and ambient pressure at 240 min.

Catalysts	Glycerol conversion (%)	Product yield (%)					Carbon selectivity (%)
		Glycolic acid	Formic acid	Acetic acid	Acrolein	Acrylic acid	
SiW/Al_2O_3	83.78	15.34	7.90	18.83	5.44	25.11	80.02
SiW/SiO_2	79.80	9.97	5.05	16.17	3.38	17.50	45.50
SiW/HZSM-5	85.54	16.95	9.53	19.51	7.47	30.57	84.03

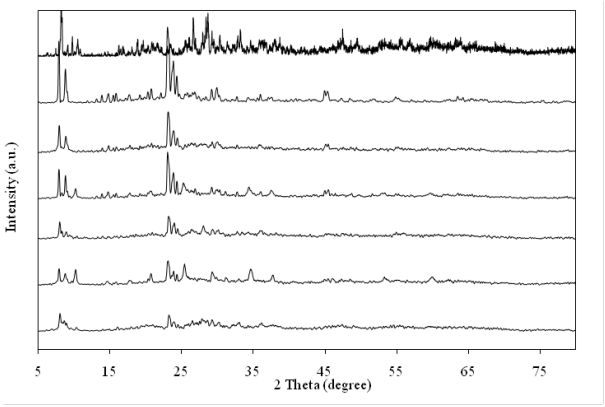

Figure 4 XRD patterns of supported SiW catalysts at different type of support (◆ SiW hexahydrate and ● HZSM-5).

surface area and high acidity of SiW/SiO_2 catalyst, where low glycerol conversion and product yield were obtained. This can be said that the BET surface area played a more important role on the activity for glycerol oxydehydration via supported SiW catalysts than the total acidity.

Effect of SiW loading

The XRD patterns of SiW/HZSM-5 samples with different SiW loadings in the range of 20-60 wt.% are exhibited in Figure 4. The XRD peaks of all SiW/HZSM-5 catalysts were intermediary between that of unsupported SiW and HZSM-5 support. Increasing the SiW loading reduced the intensity of the main characteristic peaks of HZSM-5, emerging at 2θ of 7.8°, 8.7°, 23.1°, 23.3°, 23.6°, 23.8°, and 24.3°. When the SiW loading was below 40 wt.%, the XRD patterns of SiW/HZSM-5 catalysts were still similar tothat of HZSM-5, and peak assignable to HZSM-5 was observed, which suggested that HZSM-5 was higher crystalline phase. Regarding the textural properties and surface chemistry of supported SiW catalysts at different SiW loadings, the BET surface area and pore volume diminished with the increasing SiW loading. This might be due to the agglomeration of SiW catalyst on the support surface. Namely, the generated agglomerates cannot enter the pores of the support because of the presence of diffusion resistance (Bordoloi et al., 2007). Thus, they blocked the pores, resulting in the decrease of pore volume as well as pore diameter, which led to a decline in the BET surface area (Lili et al., 2008). In addition, it also resulted in the decrease of SiW dispersion and the amount of effective acid sites as listed in Table 4.

With regard to the effect of SiW loading on the activity of supported SiW catalysts for the oxydehydration of glycerol, the similar trends of glycerol conversion and product yield along the reaction time were observed as the effect of supports (Figure S.1). Glycerol conversion increased considerably during the early period of reaction time and leveled off at reaction times longer than 120 min. The yields of acetic acid, glycolic acid and formic acid increased slightly with increasing reaction time. A high

Table 4 Textural properties and surface chemistry of supported SiW catalysts in the presence of different SiW loadings

SiW loading (wt.%)	Textural properties			Surface chemistry	
	BET surface area (m^2/g)	Pore volume (cm^3/g)	Average pore diameter (Å)	Acid amount (mmol NH_3/g Cat.)	Total acidity (mmol NH_3/g Cat.)
0	289.4a	0.173	4.32	0.71 (81-349 °C) 0.25 (362-640 °C)	0.97
20	250.2	0.164	2.62	0.87 (39-298 °C) 0.15 (39-298 °C)	1.02
30	233.4	0.153	2.62	0.88 (46-342 °C) 0.43 (546-675 °C)	1.31
40	199.13	0.135	2.72	0.90 (25-295 °C) 0.45 (530-662 °C)	1.35
50	157.25	0.110	2.80	0.89 (30-297 °C) 0.65 (527-719 °C)	1.54
60	146.41	0.102	2.79	1.83 (30-389 °C) 0.92 (515-711 °C)	2.75

[a]SiW/HZSM-5 catalyst at 90 °C and 30 wt.% SiW loading after 6 times used.

Table 5 Effect of SiW loading on the performance of glycerol oxydehydration over SiW/HZSM-5 catalysts at reaction temperature of 90 °C and ambient pressure at 240 min.

SiW loading (wt.%)	Conversion (%)	Yield (%)					Carbon selectivity (%)
		Glycolic acid	Formic acid	Acetic acid	Acrolein	Acrylic acid	
0	80.11	5.12	3.93	5.94	13.76	8.23	36.98
20	87.02	13.79	9.14	18.52	5.41	26.29	73.15
30	85.54	16.95	9.53	19.51	7.47	30.57	84.03
40	73.36	8.96	5.39	13.26	2.61	18.33	48.54
50	50.01	5.72	3.11	8.20	1.41	12.17	30.35
60	45.91	3.79	2.72	5.22	0.73	8.04	20.50

yield of acrolein was obtained during the first 30-120 min and then decreased considerably due to the oxidation to acrylic acid. At 240 min reaction time, the presence of SiW at 20 wt.% loading can enhance the conversion of glycerol from 80.1 to 87.0%, or around 1.09-fold, and can reduce the transformation of glycerol to undesired products from 63.0 to less than 26.9% (Table 5), compared that in the absence of SiW. In addition, it can facilitate a more generation of glycolic acid, formic acid, acetic acid, acrolein and acrylic acid of 2.69, 2.32, 3.12, 0.39 and 3.19-fold, respectively. The presence of SiW at 30 wt.% loading provided slightly lower glycerol conversion (85.54%) compared with that at 20 wt.% SiW (87.0%). However, it provided a higher yield of glycolic acid, formic acid, acetic acid, acrolein and acrylic acid of around 1.23, 1.05, 1.05, 1.33 and 1.16-fold, respectively. Further raising the SiW loading resulted in the decrease of either glycerol conversion or yield of desired products. In addition, it increased the conversion of glycerol to undesired species, monitoring by the carbon selectivity.

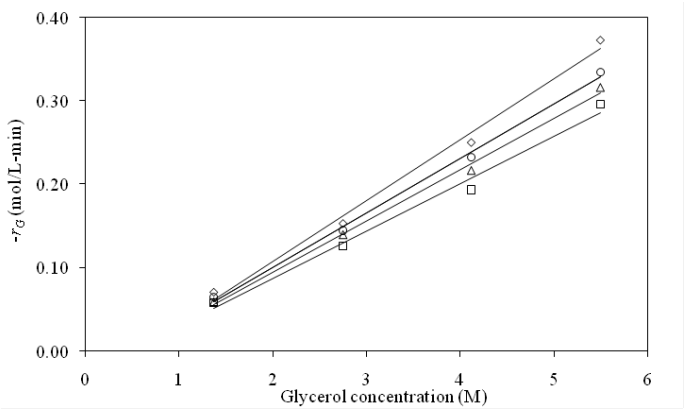

Figure 5 Variation of glycerol conversion rate as a function of glycerol concentrations in the presence of H_2O_2 at the concentrations of (□) 1.37, (△) 2.74, (○) 4.79 M and (◇) 6.85 M at 90 °C.

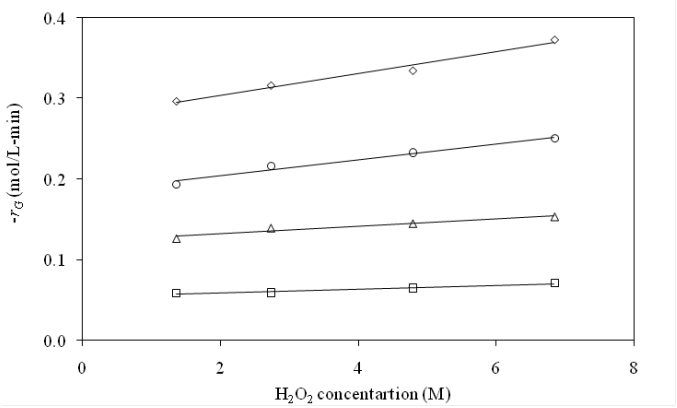

Figure 6 Variation of glycerol conversion rate as a function of H2O2 concentrations in the presence of glycerol at the concentrations of (□) 1.37, (△) 2.75, (○) 4.12 M and (◇) 5.50 M at 90 °C.

This is because the catalysts with too high acidity facilitated the conversion of glycerol to unwanted compounds, which can observe explicitly by a low carbon selectivity at SiW loading of 60 wt.%. Besides, the presence of high SiW loading can block the pores and lowered the available surface area as demonstrated in Table 4, leading to a decline in the activity of the catalyst. The similar result was also reported by the dehydration of glycerol to acrolein over activated carbon-supported SiW catalysts (Lili et al., 2008).

Kinetic studies

The kinetic of glycerol conversion was carried out via the best catalytic activity catalyst, SiW/HZSM-5 with SiW loading of 30 wt.% at different temperatures in the range of 70-90 °C. The glycerol and H_2O_2 concentrations were varied from 1.37-5.50 M and 1.37-6.85 M, respectively. As expected, the conversion of glycerol increased as the increasing reaction temperature. The data used to determine the kinetic of glycerol conversion was taken from the linear section of glycerol conversion at the conversion less than 40%.

The variations of glycerol conversion rate in the presence of different concentrations of glycerol and H_2O_2 are plotted in Figure 5. It can be seen that the concentration of glycerol affected importantly on the rate of glycerol conversion (Figure 5), while the concentration of H_2O_2 affected very slightly (Figure 6). Increasing the glycerol concentration resulted to the increase of reaction rate. By using the power law model with the rate expression as Eq.(4), the reaction orders of glycerol (a) and H_2O_2 (b) were 1.2 (ca.1) and 0.1 (ca.0), respectively.

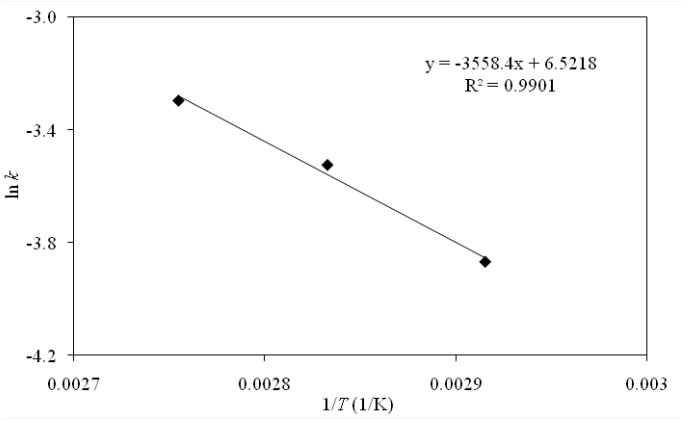

Figure 7 Arrhenius plot of rate constants for liquid phase oxydehydrationof glycerol over SiW/HZSM-5 catalyst

$$r_G = -k\,[\mathrm{G}]^a\,[\mathrm{H_2O_2}]^b \quad (4)$$

where r_G is the rate of glycerol conversion, k is the rate constant, [G] and [H_2O_2] are the concentration of glycerol and H_2O_2, respectively and a and b are the reaction order of glycerol and H_2O_2 concentrations, respectively.

According to the Arrhenius's equation (Eq.(5)), plot of rate constant versus temperature (Figure 7) provides the apparent activation energy of 29.58 kJ/mol, which is close to the activation energy reported for the glycerol oxidation over supported gold catalyst at particular oxygen pressures up to 10 bar and at temperatures from 25 to 100 °C (Bordoloi et al., 2007).

$$k = k_0\,\exp\left(\frac{-E_a}{RT}\right) \quad (5)$$

where k is the rate constant, k_0 is the frequency factor, E_a is the activation energy (kJ/mol), R is the gas constant (8.314 J/mol·K) and T is absolute temperature (K).

Conclusions

The oxydehydration of glycerol to acrylic acid was successfully performed in liquid phase at low temperature (90 °C) via supported SiW catalysts. Besides the acrylic acid, various interesting compounds were generated and measurable including glycolic acid, formic acid, acetic acid and acrolein. The presence of only H_2O_2 or only SiW cannot facilitate a satisfactory glycerol conversion and yield of desired products. The presence of both had the synergetic positive effect on glycerol conversion and product yield. The acid strength of supported SiW catalysts was in the order of SiW/Al_2O_3 > SiW/HZSM-5 > SiW/SiO_2, while the BET surface area of supported SiW catalysts was ranked in the order of SiW/HZSM-5 > SiW/Al_2O_2> SiW/SiO_2. As obviously observed, the catalytic activities foroxydehydration of glycerol werein the order of SiW/HZSM-5 > SiW/Al_2O_3 > SiW/SiO_2, suggesting that the activity of supported SiW catalysts depended significantly on the BET surface area than the acidity. The rate of glycerol conversion can be explained by a pseudo-first order reaction with respect to glycerol concentration.

Acknowledgments

The authors would like to thank the Royal Golden Jubilee (RGJ) Ph.D. Program and the Thailand Research Fund (TRF) for financial support (Grant No. PHD/0336/2551) and the Center of Excellence on Petrochemical and Materials Technology (PETRO-MAT), Chulalongkorn University and the Department of Chemical Engineering, Mahanakorn University of Technology for facility support.

References

Akiyama, M., Sato, S., Takahashi, R., Inui, K., and Yokota, M. (2009) Dehydration-hydrogenation of glycerol into 1,2-propanediol at ambient hydrogen pressure. *Applied Catalysis A: General* 371(1-2): 60-66.

Atia, H., Armbruster, U., and Martin, A. (2008) Insights in the mechanism of selective olefin oligomerisation catalysis using stopped-flow freeze-quench techniques: A Mo K-edge QEXAFS study. *Journal of Catalysis* 284: 247-258.

Beatrice, C., Blasio, G. D., Lazzaro, M., Cannilla, C., Bonura, G., Frusteri, F., Asdrubali, F., Baldinelli, G., Presciutti, A., Fantozzi, F., Bidini, G., and Bartocci, P. (2013) Technologies for energetic exploitation of

biodiesel chain derived glycerol: Oxy-fuels production by catalytic conversion. *Applied Energy* 102: 63-71.

Bordoloi, A., Vinu, A., and Halligudi, S. B. (2007) Oxyfunctionalisation of adamantane using inorganic-organic hybrid materials based on isopoly and heteropoly anions: Kinetics and mechanistic studies. *Applied Catalysis A: General* 33(1): 143-152.

Chieregato, A., Basile F., Concepción, P., Guidetti, S., Liosi, G., Soriano, M. D., Trevisanut, C., Cavani, F., and Nieto, J. M. L. (2012) Glycerol oxidehydration into acrolein and acrylic acid over W–V–Nb–O bronzes with hexagonal structure. *Catalysis Today* 197: 58-65.

Chino, N., and Okubo, T. (2005) Nitridation mechanism of mesoporous silica: SBA-15. *Microporous and Mesoporous Materials* 87(1): 15-22.

Deckwer, W. D. (1995) Microbial conversion of glycerol to 1,3 propanediol. *FEMS Microbiology Reviews* 16: 143-149.

Deleplanque, J., Dubois, J. L., Devaux, J. F., and Ueda, W. (2010) Production of acrolein and acrylic acid through dehydration and oxydehydration of glycerol with mixed oxide catalysts. *Catalysis Today* 157(1-4): 351-358.

Demirbas, A. (2009) Biodiesel from waste cooking oil via base-catalytic and supercritical methanol transesterification. *Energy Conversion and Management* 50(4): 923-927.

Etzkorn, W. G., Pedersen, S. E., and Snead, T. E. (2002) *Kirk-Othmer Encyclopedia of Chemical Technology*. John Wiley & Sons, pp. 265-288.

Ghosh, D., Sobro, I.F., and Patrick, C.H. (2012) Stoichiometric conversion of biodiesel derived crude glycerol to hydrogen: Response surface methodology study of the effects of light intensity and crude glycerol and glutamate concentration. *Bioresource Technology* 106: 154-160.

Gong, L., Lu, Y., Ding, Y., Lin, R., Li, J., Dong, W., Wang, T., and Chen, W. (2010) Selective hydrogenolysis of glycerol to 1,3-propanediol over a $Pt/WO_3/TiO_2/SiO_2$ catalyst in aqueous media. *Applied Catalysis A: General* 390: 119-126.

Guo, X., Li, Y., Shi, R., Liu, Q., Zhan, E., and Shen, W. (2009) Co/MgO catalysts for hydrogenolysis of glycerol to 1, 2-propanediol. *Applied Catalysis A: General* 371: 108-113.

Henao, C. A., Simonetti, D., Dumesic, J. A., and Maravelias, C. T. (2009) Conversion of Glycerol to Liquid Fuels. *Computer Aided Chemical Engineering* 27: 1719-1724.

Huang, Z., Cui, F., Kang, H., Chen, J., and Xia, C. (2009) Characterization and catalytic properties of the CuO/SiO_2 catalysts prepared by precipitation-gel method in the hydrogenolysis of glycerol to 1,2-propanediol: effect of residual sodium. *Applied Catalysis A: General* 366: 288-298.

Kongjao, S., Damronglerd, S., and Hunsom, M. (2011) Electrochemical reforming of an acidic aqueous glycerol solution on Pt electrodes. *Journal of Applied Electrochemistry* 41: 215-222.

Kozhevnikov, I. V. (1995) Homogeneous catalysis by transition metal oxygen anion clusters. *Catalysis Reviews: Science and Engineering* 37: 311-455.

Kunkes, E. L., Simonetti, D. A., Dumesic, J. A., Pyrz, W. D., Murillo, L. E., Chen, J. G., and Buttrey, D. J. (2008) The role of rhenium in the conversion of glycerol to synthesis gas over carbon supported platinum-rhenium catalysts. *Journal of Catalysis* 260: 164-177.

Lee, S.-H. and Moon, D. J. (2011) Studies on the conversion of glycerol to 1,2-propanediol over Ru-based catalyst under mild conditions. *Catalysis Today* 174: 10-16.

Li, F., Xue, F., Chen, B., Huang, Z., Yuan, Y., and Yuan, G. (2012) Direct catalytic conversion of glycerol to liquid-fuel classes over Ir-Re supported on W-doped mesostructured silica. *Applied Catalysis A: General* 449: 163-171.

Lili, N., Yunjie, D., Weimiao, C., Leifeng, G., Ronghe, L., Yuan, L., and Qin, X. (2008) Glycerol dehydration to acrolein over activated carbon-supported silicotungstic acids. *Chinese Journal of Catalysis* 29(3): 212-214.

Liu, Y. and Wang, L. (2009) Biodiesel production from rapeseed deodorizer distillate in a packed column reactor. *Chemical Engineering and Processing* 48: 1152-1156.

Markov, S. A., Averitt, J., and Waldron, B. (2011) Bioreactor for glycerol conversion into H_2 by bacterium *Enterobacter aerogenes*. *International Journal of Hydrogen Energy* 36:262-266.

Ning, L., Ding, Y., Chen, W., Gong, L., Lin, R., Lu, Y., and Xin, Q. (2008) Glycerol dehydration to acrolein over activated carbon-supported silicotungstic acids. *Chinese Journal of Catalysis*29(3): 212-214.

Popa, A., Sasca, V, Kis, E. E., Neducin, R. M., Bokorov, M. T., and Halasz, J. (2005) Structure and texture of some keggin type hetero-polyacids supported on silica and titania. *Journal of Optoelectronics and Advanced Materials* 7(6): 3169-3179.

Sabourin-Provost, G., and Hallenbeck, P. C. (2009) High yield conversion of crude glycerol fraction from biodiesel production to hydrogen by photofermentation. *Bioresource Technology* 100: 3513-3517.

Shen, L., Yin, H., Wang, A., Feng, Y., Shen, Y., Wu, Z., and Jiang, T. (2012) Liquid phase dehydration of glycerol to acrolein catalyzed by silicotungstic, phosphotungstic, and phosphomolybdic acids. *Chemical Engineering Journal* 180: 277-283.

Shen, L., Yin, H., Wang, A., Lu, X., and Zhang, C. (2014) Gas phase oxidehydration of glycerol to acrylic acid over Mo/V and W/V oxide catalysts. *Chemical Engineering Journal* 244: 168-177.

Simonetti, D. A., Kunkes, E. L., and Dumesic, J. A. (2007) Gas-phase conversion of glycerol to synthesis gas over carbon-supported platinum and platinum–rhenium catalysts. *Journal of Catalysis* 247(2): 298-306.

Smith, P. C., Ngothai, Y., Nguyen, Q. D., and O'Neill, B. K. (2009) Alkoxylation of biodiesel and its impact on low-temperature properties. *Fuel* 88(4): 605-612.

Thanasilp, S., Schwank, J. W., Meeyoo, V., Pengpanich, S., and Hunsom, M. (2013) Preparation of supported POM catalysts for liquid phase oxydehydration of glycerol to acrylic acid. *Journal of Molecular Catalysis A: Chemical* 380: 49-56.

Tichý, J. (1997) Oxidation of acrolein to acrylic acid over vanadium-molybdenum oxide catalysts. *Applied Catalysis A: General* 157(1-2): 363-385.

Tsukuda, E., Sato, S., Takahashi, R., and Sodesawa, T. (2007) Production of acrolein from glycerol over silica-supported heteropoly acids. *Catalysis Communications* 8: 1349-1353.

Ulgen, A. and Hoelderich, W. F. (2011). Conversion of glycerol to acrolein in the presence of WO_3/TiO_2 catalysts. *Applied Catalysis A: General* 400(1-2): 34-38.

Van de Vyver, S., D'Hondt, E., Sels, B. F., and Jacobs, P. A. (2010) Preparation of Pt on NaY zeolite catalysts for conversion of glycerol into 1,2-propanediol. *Studies in Surface Science and Catalysis* 175: 771-774.

Witsuthammakul, A. and Sooknoi, T. (2012) Direct conversion of glycerol to acrylic acid via integrated dehydration–oxidation bed system. *Applied Catalysis A: General*413-414: 109-116.

Zakaria, Z. Y., Linnekoski, J., and Amin, N. A. S. (2012) Catalyst screening for conversion of glycerol to light olefins. *Chemical Engineering Journal* 207-208: 803-81.